Modelling the engineering behaviour of fibrous peat formed due to rapid anthropogenic terrestrialization in Hangzhou, China

Z.X. Yang[1], C.F. Zhao[2], C.J. Xu[3], S.P. Wilkinson[4], Y.Q. Cai[5], K. Pan[6]

Abstract

Peat is a very variable but normally weak material. While engineering failures involving peat are common, the full diversity of engineering behaviours exhibited by peat have not been well classified due to the large range of possible compositions of peats. A laboratory study carried out on the peat at Jiangyangfan Eco-park, located in Hangzhou, China identify it as displaying an intermediate engineering response compared to the ranges normally observed for peat. The peat is a fill (made ground) originating from dredging of the West Lake, a site of cultural and historic importance in China. Given its relatively unique mechanism of deposition the distinctive characteristics of this peat are presented in comparison to other peats reported in the literature highlighting its intermediate nature. The shearing behaviour of peat can be described using the framework of critical state theory. The most prominent characteristic of the West Lake Peat is that plastic deformation occurs at very small stress levels. A constitutive model based on critical state theory for predicting the undrained shear behaviour of this type of peat from low stress to critical state level is presented. This model also includes several elements of peat behaviour previously reported and it may therefore

[1]Professor, Dept. of Civil Engineering, Zhejiang University, China, zxyang@zju.edu.cn
[2]Former postgraduate student, Dept. of Civil Engineering, Zhejiang University, China, zhaochaofa@zju.edu.cn; currently Ph.D student at Ecole Centrale de Nantes, France
[3]Professor, Dept. of Civil Engineering, Zhejiang University, China, xucj@zju.edu.cn
[4]Senior Lecturer, Department of Civil Engineering, University of Wolverhampton, Wulfruna Street, WV1 1LY, UK, S.wilkinson4@wlv.ac.uk
[5]Professor, Department of Civil Engineering, Zhejiang University, caiyq@zju.edu.cn
[6]Postgraduate student, Dept. of Civil Engineering, Zhejiang University, China, pk2013@zju.edu.cn

be applied to a wider range of peat soils.

Keywords: Peat; physiochemical properties; compression; undrained shear; critical state; constitutive model

Introduction

Peat is the most variable soil type with respect to engineering purposes. It is defined as a predominantly organic soil which accumulates in-situ in a mire (BS 5930, 1999). However peats and peaty soils can develop in a very wide range of geotechnical environments. In addition to organic components, peats can contain the full range of constituents also found in mineral soils depending on the conditions under which the peat has been formed. The organic components of peat can also vary widely in terms of both origin and geotechnical behaviour. In engineering peats are classified as ranging from fibrous peats, where the organic constituents remain largely identifiable, to amorphous peats where the original structure of the organic components have either been lost due to decomposition, or where the peat was originally deposited as a sludge (BS EN ISO 14688-1, 2002). Within this broad spectrum there is a large potential for variation in response to the range of organic components from which the peat is formed. One of the more commonly used classification systems for peat, presented by Hobbs (1986), uses twelve distinct scales for each of twelve peat descriptors. Given all of the possible options within this system, a very large set of unique peat classifications can be generated. While some combinations are unlikely in practice, the term peat still encompasses a substantial range of materials with an equally wide range of engineering behaviours. One of the most important factors controlling the engineering behaviour of peat is the content of organic fibres. Fibres provide tensile strength, and the amount of fibres in a peat is critical for its overall behaviour.

Peat is often described in the literature as a very soft and problematic engineering material. Peats often have very high void ration and water content, resulting in very low initial values of bulk density. As a result peats often exhibit high values of compressibility, and are commonly reported as responsible for excessive amounts of observed settlement (Berry and Poskitt 1972, Edil et al 1991, Nichol and Farmer 1998, Mesri and Ajlouni 2007, Kazemian et al 2011, Zhang and O'Kelly 2014). Many geostructures such as slopes, embankments, retaining walls and foundations which have been constructed on peat have experienced damage or stability issues (Mesri and Choi 1985, Long 2005, Kværner and Snilsberg 2008, Zwanenburg et al 2012, Boylan and Long 2014). In the majority of models for simulating peat behaviour effective stress based approaches is commonly used directly (Yamaguchi et al 1985, Long and Jennings 2006, den Haan and Grognet 2014). This approach assumes that soil particles are incompressible. Peats have a high proportion of organic particles which often have high intra-particle water contents. As these particles can compress, deform and change their intra-particle moisture content the assumption of incompressible particles is likely not valid. On this basis the applicability of the effective stress based approach has recently been brought into question (Zhang and O'Kelly 2014). When modelling peat engineering behaviour it is important to simulate its viscous nature including its dependency on deformation rate and its long term deformation capacity. Secondary consolidation in peat is often much more significant than for other geomaterials (Mesri et al 1997, Kramer 2000, Mesri and Ajlouni 2007). In comparison to inorganic/clastic soils, peats commonly display high values of undrained shear strength and much higher effective friction angles (Yamaguchi et al 1985, Long 2005, Cheng et al. 2007, Mesri and Ajlouni 2007, Hendry et al 2012, O'Kelly and Zhang 2013). This is especially true for peats with a reasonably large quantity of constituent fibres or fragmented plant tissues.

A wide range of geotechnical materials have been successfully modelled using critical state theory, but very few attempts to characterize peat using this approach have been made. This is likely because samples are not sheared to critical state failure because samples normally undergo tensile failure prior to reaching critical state due to the high frictional strength of peat. However, recently effort has been made to understand peat behaviour within the critical state framework. Boumezerane (2014) adopted a critical state based kinematic model to simulate the unloading/reloading behaviour of peat, and den Han and Feddema (2013) analysed the deformation and strength of embankments on soft Dutch peat using a viscous version of the modified Cam-clay framework. These successes indicate that there is a potential that critical state based approaches could be used to improve the understanding of the engineering behaviour of peats and highly organic mineral soils. The engineering behaviour observed from the peat samples, in addition to the range of previously observed engineering behaviours of peats from across the world indicates the range of behaviours that samples of peat can display.

This paper presents a laboratory study of the behaviour of peat obtained from the Jiangyangfan Eco-park (originally dredged from the nearby West Lake) which is a wildlife preserve within the city of Hangzhou, China. The West Lake peat is a fibrous material but with a relatively low number of coarse fibres. A modified constitutive model based on a critical state framework and concepts of dilatancy for simulating the undrained engineering behaviour of this peat during shear failure is presented. Model applicability and accuracy is evaluated by comparison with experimental results for the West Lake Peat sheared under undrained conditions with varying initial consolidation stresses.

Field site

In 2008, the construction of an eco-park was initiated to develop the vacant Jiangyangfan site (Fig. 1), 3km to the south of West Lake (also known as Xihu) near Hangzhou in Zhejiang Province, China, as part of the West Lake Cultural Landscape, which was inscribed on UNESCO's World Heritage List in 2011. Prior to 1999 the site was the Jiangyangfan reservoir, however it was selected as the repository for materials dredged from the West Lake. The West lake has been dredged by pipeline three times during its history in 1952, 1976 and 1999 respectively (Hangzhou local Chronicles compilation committee, 2003). Prior to this date the lake had been dredged many times by hand during its history. In fact the first time the lake is referred to in an official document using its current name West Lake ("Xihu") was in relation to a request for dredging in the year 1090 by the famous poet Su Shi (1090), the then governor of Hangzhou. This request refers to an even earlier dredging event performed around year 821-824. Dredging of the lake is thus a major element of the local history and culture. Prior to 1952 the lake had reached a very bad state with water depth reduced to about 0.5m due to build-up of organic sludge. Leaves and vegetation had accumulated in the lake along with clay and silt generating a material rich in organic matter at a very high moisture content. It was then decided that the lake would undergo periodic dredging to remove this sludge via temporary pipelines (Shao et al 2007). During the most recent dredging carried out between 1999 and 2003 the sludge was excavated and pumped along an approximately 4km long pipeline between West Lake and Jiangyangfan reservoir. During transportation the sludge was mixed with large volumes of water, and thus its original fabric was completely disrupted. During the four years of dredging approximately 1,000,000 m^3 of sludge was removed to Jingyangfan reservoir. The materials completely terrestrialized the reservoir leaving only a few surface ponds of water between small hillocks of settling dredged material. The peat at Jiangyangfan covers an area of over 100,000 m^2 and fills the contours of the original reservoir going down to a depth of approximately 18m at the deepest point (Fig. 2). After the completion of the dredging in 2003 the site was left undisturbed during which time it underwent consolidation under its own self-weight until 2008 when construction of the Jiangyangfan Eco-park commenced. Fig. 3 shows aerial views of Jiangyangfan Eco-park site during the period from 2000-2015.

Due to the difficult foundation conditions, construction of the main buildings took 2 years. Across the rest of the park pedestrian walkways were constructed on floating footings. Some covered pavilions and pagodas were built to allow tourists to observe birds and wildlife that have colonised the wetland. At an early stage concerns were raised over the potential for excessive settlement within the park, and so following construction the site was monitored; at present settlements of over 700mm have been observed. The systematic experimental investigation outlined below was carried out to better understand the causes of the observed excessive settlement, to assist with remedial works on the current pedestrian walkways and to aid the foundation design of future building/structures in and around the eco-park.

Samples were obtained using a thin-wall sampler and taken to the laboratory for further testing. The peat is known as West Lake Peat (WLP) as it was originally deposited within the West Lake. Considering that the formation process of the WLP within Jiangyangfan Eco-park is very different from the formation process followed by most other peat deposits, its basic physical properties, mineral composition, micro-structure, and mechanical behaviour are all presented. The tests outlined below were performed on reconstituted peat samples except where specified.

Peat mineralogy composition and index properties

The WLP samples were dark brown and had a slight organic smell. The index and physico-chemical properties of WLP are summarized in Table 1. The water content of the peat was determined by oven-drying the specimens at a temperature of 65^{o}C for 48 hours following the National Standard of China (SSTE 1999) procedure. The initial water content w_0 of the natural peat varies in the range of 320-400%, whereas the reconstituted samples have a mean initial water content w_0 of 182%. The ignition loss (N) was determined by combustion at 700^{o}C for 7 hours as suggested by SSTE (1999) giving an ignition loss of 35%. Sempton and Petley (1970) suggested that organic matter content (OC) and loss on ignition are approximately equivalent, such that the same values of *N* and *OC* are assumed for WLP in this study.

As organic matter has a lower specific gravity G_s than most minerals, the specific gravity (solids density) of peats and organic soils is usually less than those for inorganic soils (2.65-2.76 g/cm^3). The pycnometer method was used to determine the peats specific gravity, and the mean value obtained was 2.12 g/cm^3. G_s can be predicted from N using (den Haan and Kruse 1986),

$$\frac{1}{G_s} = \frac{N}{1.354} + \frac{1-N}{2.746} \qquad \text{Eq. (1)}$$

Substituting N=0.35 into above equation yields G_s=2.02, which is very close to the measured value of 2.12 (Table 1). The permeability of peat is measured by a standard constant head flow test using a permeameter (SSTE 1999) and is about 2.4×10^{-8} cm/s at a vertical load of σ'_v =50 kPa and falls to 1.83×10^{-8} cm/s when σ'_v increases to 200 kPa.

Classification of peat

Two major systems exist for the classification of peat: the von Post (1922) system and the Radforth (1969) system. At present both systems are widely used. From an engineering perspective the von Post system has several advantages, its definition of the peats degree of humification, which ranges from H_1 for intact, young peat to H_{10} for completely decomposed peat, provides a good general idea of the state of the peat. The von Post system also describes water content, and the content of fine and coarse fibres, wood and plant remnant, all of which contribute towards the engineering behaviour of the peat. Hobbs (1986) suggested that the von Post classification system should be further extended and so proposed the modified von Post system through introducing categories for organic content, anisotropy, tensile strength, odour, plasticity and acidity. This modified von Post classification is very useful for engineering purposes because it covers most physical and mechanical features of a peat and so this system was used during this study.

In the system extended by Hobbs (1986), each classifier is designated by a letter, and the degree to which the characteristic is presented, is designated by an index. The rules for classification presented in this paper are those of von Post (1922) and extended by Hobbs (1986). Using this system, the WLP at Jiangyangfan Eco-park is classified as: B H_6 B_2 F_2 R_1 W_0 (von Post, 1922) / N_1 TV_2 TH_2 A_1 P_1 pH_L (extension proposed by Hobbs, 1986). This designates the WLP as Bryales moss peat with a moderate degree of humification (H), water content less than 500% (B), a high but not predominant fibre content (F), a low content of coarse fibres (R), no wood (W), organic content 20% to 40% (N), moderate tensile strength in the vertical direction (TV) and horizontal direction (TH), slight smell (A), a detectable plastic limit (P) and acidity (pH).

Microstructure

An electron microscope investigation was carried out using a Hitachi TM 3000 tabletop microscope to analyse the microsctucture of the reconstituted WLP. The samples were prepared by oven-drying, then they were mounted on 5mm aluminium stubs with double sided sticky carbon tabs to ensure good conductivity between the sample and the stub. The samples were then placed into the Scanning Electron Microscope (SEM). Samples were imaged uncoated but at a relatively low vacuum to reduce the potential for charge build-up. Some details of the SEM preparation techniques used for this peat are described in Wilkinson (2011). Figures 4(a)-(f) are SEM micrographs of WLP. Fig. 4(a) shows the overall nature of the microstructure of the WLP, being a mixture of plant fibre networks and siliciclastic particles with some evidence of larger void spaces. The peat contains a few stem structures (Fig. 4(b)-(d)) and decayed leaves on which a few stomal pores are visible as small dimples in the leaf's otherwise smooth surface (Fig. 4(e)). In addition pyritic framboids were observed in the soil suggesting relatively low oxygen concentrations within the peat (Fig. 4(f)). It is likely that the fibrous elements (Fig. 4(b-c)) could enhance the shear strength of the peat especially as they are irregularly arranged (Fig. 4(d)).

One-dimensional compression tests

One dimensional compression tests were carried out to investigate the consolidation/settlement behaviour of the WLP. Pichan and O'Kelly (2012) showed that the compressional behaviour of peat depends on its degree of decomposition which relates to the degree of humification within the von Post classification system outlined above. The degree of decomposition of a peat is affected by environmental factors including temperature, oxygen supply, pH, C:N ratio (carbon to nitrogen), and organic constituents, etc. For the WLP the initial void ratio of the natural peat varies between 6.78 and 8.48 (Table 1), and the reconstituted sample has a mean initial void ratio e_0=3.86. One-dimensional compression tests were performed on reconstituted samples (20mm in height and 61.8mm in diameter) using a conventional oedometer. A standard series of load increments were employed for the test: 12.5kPa, 25kPa, 37.5kPa, 50kPa, 75kPa, 100kPa, 150kPa, 200kPa, 250kPa, 300kPa, 350kPa, 400kPa, 450kPa, 600kPa, and 800kPa. Each loading step lasted for 24 hours. Fig. 5(a) shows the cumulative axial strain with elapsed time for the first three loading steps, and Fig. 5(b) shows the compression curve of the reconstituted peat sample.

Not surprisingly, the immediate compression is high, especially at high load levels, due to the large void ratio and high compressibility. For the 25kPa and 50kPa loads, the immediate axial strain is approximately 11% and 19%, which is much higher than the accepted settlement limit for normal buildings or structures. At 50kPa, the total axial strain is about 28% The e-log(σ_v) curves continue to decrease even after 24 hours (Fig. 5(a)), indicating a significant amount of secondary consolidation. A linear trend is observed between void ratio e and log(σ_v) when σ_v >12.5kPa (Fig. 5(b)), with a compression index of c_c=1.23, identifying WLP as highly compressible. The secondary compression index c_α is defined by the slope of the final part of the compression curve, and is measured as the unit compression over one decade on a log time scale, i.e. c_α=de/dlog(t). Based on a 24 hour standard oedometer test, the measured mean c_α is about 0.07~0.10 at σ_v=12.5-50 kPa. The ratio of c_α/c_c represents the deformability of soil particles. Peat deposits with highly deformable organic matter normally have greater values for c_α/c_c, in comparison to granular media composed of less deformable siliciclastic particles. The ratio of c_α/c_c=0.056-0.081 for the WLP compares well with the normal expected range of 0.06±0.01 for peat deposits given by Mesri et al (1997) and Mesri and Ajlouni (2007). Mesri et al (1997) also observes that fibrous peats display the highest c_α/c_c values of all geotechnical materials. The results from the fibrous WLP are, thus in full agreement with this observation.

Undrained triaxial compression tests

Undrained triaxial tests were performed using a standard triaxial testing system, capable of performing a variety of functions including isotropic and anisotropic consolidation and various modes of shear loading. Reconstituted peat specimens were prepared and consolidated using a specially designed consolidation apparatus for peat (Fig. 6). Large inclusions including roots and pieces of gravel were removed before placing the peat into the 150mm diameter 350mm height sample preparation acrylic tube. The sample was then subjected to vertical compression under a confining stress of 30 kPa until a settlement rate less than 0.005mm/hour was observed, which usually occurred after approximately 120 hours. The compressed sample was pushed out of the tube and trimmed to a length of 140mm and a diameter of 70mm for consolidated undrained (CU) triaxial testing. In total, five reconstituted specimens were prepared at initial effective confining stresses ranging from 30 to 200 kPa.

A back pressure of 200 kPa was applied to all CU test specimens to achieve full saturation, which was confirmed by checking that the Skempton B values were greater than 0.98. The specimens were then isotropically consolidated to the desired value of confining pressure and then a strain controlled undrained triaxial shear test was conducted at a speed of 3% strain per hour. As suggested by Jardine (2013), ageing periods were imposed during the consolidation stage prior to the samples being sheared. During each step, the residual creep rates were reduced to <1% of those that would be developed in the shearing stage. As a result, each sample was consolidated for about 6 days before being sheared to critical state which occurred at a strain of 20% for triaixial compression. The axial load was measured using a load cell and the axial displacement was measured using a linear variable differential transformer (LVDT).

Fig. 7 summarizes the results of CU triaxial tests on reconstitutedpeat specimens. The specimens display predominately strain-hardening behaviour up to large deformations (Fig. 7(a)), with the exception that slight strain-softening responses were observed for the higher initial effective stresses p'_0=100 and 200 kPa. In q-p' stress space (Fig. 7(b)), the undrained contractive behaviour is primarily seen from the increase in q during strain-hardening accompanied by a decrease in p' for all specimens. It is also noted that during the later stage of shearing, all specimens exhibit apparent volumetric dilation after passing through the phase transformation state, where the peats behaviour changes from 'contraction' to 'dilation' as is normally observed in sand samples (Ishihara et al 1975). To assist in defining the failure behaviour, the 'tension cut-off' with an inclination q/p'=3 through the origin is also plotted in the q-p' plane, which signifies a zero effective stress condition. The stress paths are all below this line, indicating that no tensile failure occurs for the WLP samples. Critical state failure is identified for these specimens when the axial strain ε_a reaches approximately 20% (Fig. 7(a)). 'Tension cut-off' failures under triaxial compression are commonly observed in peat, especially for fibrous peat samples (den Hann and Kruse 2007, Mesri and Ajlouni 2007, Zwanenburg et al. 2012). The lack of a 'tension cut-off' failure in the WLP is possibly due to the relatively low fibre content in the WLP (35%) in comparison to other peats. Although some fibres may break in tension, the frictional shear component controls the overall engineering behaviour of this fibrous peat. This type of behaviour is also observed by Yamaguchi et al. (1985) and Cola and Cortellazzo (2005). This suggests that the content and type of organic fibres will determine the failure mechanism and behaviour of fibrous peats during engineering works.

The critical state of the peat is approximated by the state of the specimens at 20% axial strain at which the rate of change of effective mean normal stress and deviatoric stress becomes insignificant (Fig. 7). The estimated critical state can be represented by the critical state lines (CSL) in a *q*-$p^{'}$ plane and an *e*-log $p^{'}$ plane, as shown in Fig. 8 (a) and (b) respectively. In the *q*-$p^{'}$ plane (Fig. 8(a)), the soil approaches a unique CSL regardless of its initial states. The critical stress ratio is 1.948, giving a critical state friction angle of 47.3°, which is much higher than those for mineral soils due to the shear resistance caused by organic fibres. Similar observations have been reported by Yamaguchi et al (1985), Long (2005), Mesri and Ajlouni (2007), Hendry et al (2012), O'Kelly and Zhang (2013). In Fig. 8(b), the critical state points can be fitted onto a straight line with a slope of 1.225. The initial states of shearing after isotropic consolidation are also shown in this figure, and they can be fitted onto an isotropic consolidation line (ICL) with a slope of 1.139.

The WLP has a distinctive effective stress path in the *q*-$p^{'}$ plane. From a very early stage of shearing with small stress ratios $q/p^{'}$, $p^{'}$ decreases due to the build-up of pore water pressure (Fig. 7(b)), leading to an inclined effective stress path on which the tangential line of the effective stress path at $p^{'}$=0 is not vertical. Similar observations are also reported by Yamaguchi et al (1985), Cola and Cortellazzo (2005), Cheng et al (2007), Hendry et al (2012), and Zwanenburg et al. (2012). This suggests plastic deformation could occur for fibrous peats like WLP at very small stress ratios. In the conventional framework of elastoplasticity, the slope of the initial effective stress path in the $p^{'}$-*q* plane can be employed to identify the elastic or elastoplastic response of materials. If the soil exhibits purely elastic behaviour under undrained conditions, the $d\varepsilon_v^p = 0$, and thus $d\varepsilon_v^e = 0$ as $d\varepsilon_v = d\varepsilon_v^e + d\varepsilon_v^p = 0$; then $d\varepsilon_v^e = dp^{'} / K = 0$, where $d\varepsilon_v$ is the volumetric strain increment with superscripts 'e' and 'p' signifying elastic and plastic and K is bulk modulus, and therefore no change of p' occurs, resulting in the tangential line of the effective stress path at p'=0 being perpendicular to the p' axis. This type of effective stress path is observed in undrained triaxial compression shear test on both sands and normally consolidated clays (Fig. 9), which is confirmed by the small strain behaviour of clays and sands investigated extensively with high-resolution triaxial experiments by Vucetic and Dobry (1988, 1991), Smith et al. (1992), Kuwano and Jardine (2007). Some peats, reported in the literature also display purely elastic behaviour at small stress ratios similar to the behaviour of mineral soils, e.g. those reported by Long (2005), den Haan and Kruse (2007), Mesri and Ajlouni (2007). The reason for these two distinctive behaviours for different peats at very small stress ratios is related to the composition of the peats. The exact elements of the peats which cause this have not been fully understood. However, this again highlights the range of compositions of peat soils which generates the range of observed engineering behaviours.

To further verify that plastic deformation occurs in the WLP occurring at the start of shearing, cyclic undrained triaxial compression tests with low amplitudes q_{cyc}=5 kPa and p'_0=50 kPa were performed with both Toyoura sand and the WLP samples. The loading programme is shown in Fig. 10(a). Fig. 10(b) compares the stress paths of peat and sand in the first loading cycle. As expected, the stress path for the sand is almost vertical in the first cycle without generating any pore pressure, in comparison the WLP is not vertical, with a net pore pressure of 5 kPa generated in the first cycle. Fig. 10(c) presents the accumulative axial strains in the first cycle. Nearly 0.06% axial strain takes place in the first cycle for the WLP, while no discernable strain is produced for the sand. Similar observations are confirmed by dynamic triaxial tests on peats at small strain carried out by Boulanger et al. (1998), Kramer (2000), Wehling et al. (2003), in which purely elastic, linear and non-hysteretic responses were not observed, even at extremely small stress/strain levels, such as would be seen in other siliciclastic soils. This behaviour of the peat forms one of the key elements of the constitutive model presented in the following section.

A simple triaxial compression model

During the last several decades, critical-state soil mechanics (Schofield and Wroth 1968) has been extensively used to model the behaviours of both sand and clay (Li and Dafalias 2000; Ling and Yang 2006; Kaliakin and Dafalias 1990; Schofield and Wroth 1968). For example, Li and Dafalias (2000) proposed a state-dependent dilatancy model for sand, which is capable of describing sand behaviour at different initial densities and under different initial confining pressures with a single set of model constants. Given the advantage of Li and Dafalias' model, it was adopted to simulate the undrained triaxial compression behaviour of WLP.

The critical state line in the e-p' plane can be expressed as (Li and Wang 1998)

$$e_c = e_\Gamma - \lambda_c (p' / p_a)^\xi \quad \text{Eq. (2)}$$

where e_c is the critical state void ratio corresponding to p', and e_Γ, λ_c and ξ are three material constants for critical state line. Using this equation, the state parameter ψ proposed by Been and Jefferies (1985) can be obtained as

$$\psi = e - e_c \quad \text{Eq. (3)}$$

where e is the void ratio at the current state. The sign of ψ can be used to determine the state of the soil considering the influence of both density and pressure (Been and Jefferies

1985; Li and Dafalias 2000).

As shown in Fig. 7, the critical state of the WLP is approximated by the state of the specimens at approximately 20% axial strain at which the rate of change of both deviatoric and mean normal effective stresses becomes insignificant. Under undrained conditions, it is assumed that plastic deformation can only occur when the stress ratio η=q/p$^{'}$ exceeds its historic maxima for virgin loading, and no plastic deformation will be produced along a constant η stress path. This assumption is approximately true for sand, as no significant volume change is induced for a constant stress ratio η under normal confining stress levels, before particle breakage occurs. However, for clay and peat, considerable volumetric deformation is observed due to consolidation, and thus the plastic deformation which occurs along a constant η stress path cannot be neglected. In this study, given that only undrained triaxial tests were performed, no yielding occurs due to increases in $p^{'}$. Thus this assumption is still valid. The yield criterion can be written as (Li and Dafalias 2000)

$$f = q - \eta p^{'} = 0 \qquad \text{Eq. (4)}$$

The condition of consistency of the yield function of Eq. (4) can be expressed as:

$$df = \frac{\partial f}{\partial p^{'}} dp^{'} + \frac{\partial f}{\partial q} dq - \langle L \rangle K_p = 0 \qquad \text{Eq. (5)}$$

in which K_p is the plastic modulus and L is the loading index defined as

$$L = \frac{1}{K_p} \left(\frac{\partial f}{\partial p^{'}} dp^{'} + \frac{\partial f}{\partial q} dq \right) = \frac{dq - \eta dp^{'}}{K_p} = \frac{p^{'} d\eta}{K_p} \qquad \text{Eq. (6)}$$

An associated flow rule is applied in deviatoric space, such that

$$d\varepsilon_q^p = \langle L \rangle \frac{\partial f}{\partial q} = p^{'} d\eta / K_p \qquad \text{Eq. (7)}$$

where $\langle\,\rangle$ is the Macauley bracket such that $\langle L \rangle = L$ for $L > 0$ and $\langle L \rangle = 0$ when $L \le 0$.

By applying a dilatancy relation, the plastic volumetric strain increment can be written as

$$d\varepsilon_v^p = Dd\varepsilon_q^p = D\langle L\rangle \frac{\partial f}{\partial q} = Dp^{'} d\eta / K_p \qquad \text{Eq. (8)}$$

Where, the following dilatancy function is proposed,

$$D = d_0 (e^{m\psi} - \sqrt{\eta / M}) \qquad \text{Eq. (9)}$$

In which d_0 and m are two material constants for the dilatanty equation and M is the critical stress ratio. Eq. (9) is slightly different from the one employed by Li and Dafalias (2000) for fine tuning the performance of their model. It can be seen that at the critical state, ψ=0 and η=M, the dilatancy D is zero according to Eq. (9), which satisfies the requirement for the critical state. More importantly, this equation can also describe both positive and negative dilatancy, depending on the state of the soils which is characterized by the state parameter ψ.

The elastic strain increments can be obtained through linear elasticity as

$$d\varepsilon_v^e = dp^{'} / K \quad \text{and} \quad d\varepsilon_q^e = dq / 3G \qquad \text{Eq. (10)}$$

in which $d\varepsilon_v^e$ and $d\varepsilon_v^p$ are elastic and plastic strain increments respectively; G and K denote the elastic shear and bulk moduli respectively. As the elastic properties of soils are normally pressure sensitive, G can be expressed by an empirical formula as follows,

$$G = G_0 F(e)(p^{'} p_a)^{0.5} \qquad \text{Eq. (11)}$$

in which G_0 is a dimensionless material constant and can be determined by resonant column tests; p_a is the atmospheric pressure for normalization; $F(e)$ is a function of the current void ratio e with a typical form of (Hardin and Richart 1963; Richart et al 1970; Iwasaki and Tatsuoka 1977)

$$F(e) = \frac{(2.97 - e)^2}{1 + e} \qquad \text{Eq. (12)}$$

The bulk modulus *K* can be expressed as

$$K = G\frac{2(1+\nu)}{3(1-2\nu)} \qquad \text{Eq. (13)}$$

where ν is Poisson's ratio of soils and for simplicity, can be treated as a material constant independent of the pressure.

Noting the additive decomposition of the strains $d\varepsilon_v = d\varepsilon_v^e + d\varepsilon_v^p$ and $d\varepsilon_q = d\varepsilon_q^e + d\varepsilon_q^p$, and by combing Eqs. (7) - (9), we can obtain the incremental stress-strain relation in triaxial space,

$$\begin{Bmatrix} dq \\ dp' \end{Bmatrix} = \Lambda \begin{Bmatrix} d\varepsilon_q \\ d\varepsilon_v \end{Bmatrix} \qquad \text{Eq. (14)}$$

where Λ is the elastoplastic stiffness matrix and can be explicitly expressed as

$$\Lambda = \left[\begin{pmatrix} 3G & 0 \\ 0 & K \end{pmatrix} - \frac{h(L)}{K_p + 3G - K\eta D} \begin{pmatrix} 9G^2 & -3KG\eta \\ 3KGD & -K^2\eta \mathrm{D} \end{pmatrix} \right] \qquad \text{Eq. (15)}$$

where $h(L)$ is the Heaviside step function, with $h(L > 0) = 1$ and $h(L \le 0) = 0$.

The plastic modulus is defined to capture the hardening and softening of soil responses under shear loading. Given the lack of information from observed plastic hardening behaviour associated with microstructural evolution, the plastic modulus K_p can also be defined as a function of the stress ratio η and state parameter ψ,

$$K_p = Gh(M - \eta e^{n\psi}) = Ghe^{-n\psi}(Me^{n\psi} - \eta) \qquad \text{Eq. (16)}$$

where *h* and *n* are two positive model constants; the elastic modulus *G* serves as a reference, rendering *h* dimensionless. Eq. (16) is a modified version of that employed for modelling sands by Li and Dafalias (2000), which is intended to model the exact response at stress ratio

η=0. It is seen that Eq. (16) inherits the merits of its original form for sand. For example, at the critical state, ψ=0 and η=M, which result in $K_p=0$, such that $d\eta / d\varepsilon_q^p = 0$, which coincides with the condition of perfect plastic flow at the critical state. In addition: 1) K_p can be positive or negative, depending on the value of ψ, such that it can describe a hardening or softening response during shearing; 2) K_p used by Li and Dafalias (2000) will become infinite when η=0, indicating that no plastic deviatoric strain occurs, nor is there any plastic volumetric strain. This holds true for most normally consolidated soils, which have a purely elastic response with a non-zero, small dη at η=0, resulting in $d\varepsilon_q^p = 0$ and such that $d\varepsilon_v^p = 0$. $d\varepsilon_q^p = 0$ yields an isotropic deformation, while $d\varepsilon_v^p = 0$ suggests that the tangent of the effective stress path in the q-p' will be vertical, and no change in the effective p' is allowed to take place under undrained conditions. However, for WLP, the effective stress path bends towards the reduction in effective stress p' right from the starting point at η=0 (Fig. 7b), and there is no purely elastic zone as discussed before.

The model variable h in Eq. (16) is found to be void ratio (e)-dependent, and a simple linear relation is proposed by Li and Dafalias (2000) as

$$h = h_1 - h_2 e \qquad \text{Eq. (17)}$$

where h_1 and h_2 are two material constants. Eq. (18) has integrated the influence of the soil density over a wide range of variation. As noted by Li (2002), an e-dependent function is used rather than a ψ-dependent function, because a change either in e or p' will alter ψ, while the influence of p' has been accounted for by the elastic shear modulus G in Eq. (11).

Model calibration and responses

In total, 11 material constants should be calibrated and used in this model. These constants can be grouped into four categories (Table 2) according to their functions. The critical stress ratio M is obtained by fitting the results of triaxial compression tests in the q-p' plane in Fig. 7(a). Parameters e_Γ, λ_c, and ξ are determined by fitting the test data with linearization of the critical state line in the e-p' plane with Eq. (2), which is shown in Fig. 11 (Li and Wang 1998). The elastic, dilatancy and hardening parameters can be calibrated and adjusted finely to fit the test data, using the calibration procedure described in Li and Dafalias (2000). All resulting constants are presented in Table 2.

In general, the model simulations compare well with the experimental results (Fig. 12). the model is able to simulate the response of WLP at low stress ratio levels, where the effective stress paths bend towards the reduction of the effective stresses in the q-p' plane (Fig. 12(a)). The model can also capture the stress-strain responses from small strain levels up to the critical state (Fig. 12(b)). Slight discrepancies are observed at very low strain levels. These are probably related to the uncertainties associated with the accurate measurement of the true small strain behaviour of undisturbed peat, and the uncertain behaviour of deformable organic particles at these small strains.

Conclusions

The following five main conclusions flow from the work described above:

1. The West Lake Peat (WLP) investigated in this study is similar in many ways to typical peats: it has a relatively high water content and low bulk density, it is highly compressible and its secondary compression is significant. However, although the fibre

content of WLP is significant it is not dominant.

2. The undrained shear behaviour of WLP can be described using critical state theory. No ‘tension cut-off’ failure was observed prior to occurrence of critical state failure, which is primarily due to its relatively low fibre content. In addition, the WLP has a higher critical state friction angle of approximately 47.3^{o}, which is much higher than those of mineral soils and is normally caused by the reinforcing effect of fibres in peats.
3. The most prominent observation of the WLP is that plastic deformation occurs at very small stress levels. The feature is very similar to the behaviour of many peats worldwide, while most mineral soils behave elastically under similar low stress ratios.
4. A constitutive model is presented that has simulative capability in predicting the undrained shear behaviour. The model response compares well with the experimental results from the beginning of shearing through to critical state failure.
5. Given that the WLP has intermediate behaviour in comparison to other peats, this model has sufficient flexibility to describe the behaviour of a wide range of peats.

The results of this study provide a fundamental basis for understanding the engineering behaviour of the WLP in Jiangyangfan Eco-park. It has been used to inform the remedial works for existing structures and foundation works for future buildings/structures in the park. At the broader scale this work provides another case study of the behaviour of a peat and highlights the wide variety of potential behaviours of this diverse and variable geotechnical material.

Acknowledgments

The research described was funded by the Natural Science Foundation of China (Grant Nos. 51322809, 51578499), Qianjiang Manage Office of Hangzhou Administration Bureau of Gardens, the National Key Basic Research Program of China (No. 2015CB057801). Their support is gratefully acknowledged. Gratitude is also extended to Dr XS Li, for insightful discussions and constructive comments on the constitutive modelling of peat.

References

Been, K., and Jefferies, M.G. (1985). A state parameter for sands. Géotechnique, 35(2), 99-112.

Berry, P.L., and Poskitt, T. J. (1972). The consolidation of peat. Géotechnique, 22(1), 27-52.

British Standards Institution, 1999. Code of practice for site investigation, BS 5930:1999. Her Majesty's Stationary Office, London.

British Standards Institution, 2002. Geotechnical investigation and testing — Identification and classification of soil, BS EN ISO 14688-1: 2002. Her Majesty's Stationary Office, London.

Boulanger, R.W., Arulnathan, R., Harder, L.F.Jr., Torres, R.A., and Driller, M.W. (1998). Dynamic properties of Sherman Island peat. Journal of Geotechnical and Geoenvironmental Engineering, 124(1), 12-20.

Boumezerane, D. (2014). Modeling unloading/reloading in peat using a kinematic bubble model. Numerical Methods in Geotechnical Engineering, Hick, Bringreve & Rohe (Eds), Taylor & Francis Group, London, 1, 9-14.

Cheng, X.H., Ngan-Tillard, D.J.M., and den Haan, E.J. (2007). The causes of the high friction angle of Dutch organic soils. Engineering Geology, 93(1), 31-44.

Cola, S., and Cortellazzo, G. (2005). The shear strength behaviour of two peaty soils. Geotechnical and Geological Engineering, 23(6), 679-695.

den Haan, E.J., and Kruse, G.A.M. (2007). Characterisation and engineering properties of Dutch peats. In Proceedings of the Second International Workshop of Characterisation and Engineering Properties of Natural Soils, Singapore, 29, 2101-2133.

den Haan, E.J., and Grognet, M. (2014). A large direct simple shear device for the testing of peat at low stresses, Géotechnique Letters, 4, 283-288.

den Haan, E.J., and Feddema, A. (2013). Deformation and strength of embankments on soft Dutch soil, Proceedings of the ICE-Geotechnical Engineering, 166(GE3), 239-252.

Edil, T.B., Fox, P.J., and Lan, L.T. (1991). Observational procedure for settlement of peat. Proc. Geo-Coast, 91, 165-170.

Hangzhou local Chronicles compilation committee (2003). Chronicles of Hangzhou. http://www.hangzhou.gov.cn/main/zjhz/hzsz/index.jsp (in Chinese).

Hardin, B.O., and Richart, F.E. (1963). Elastic wave velocities in granular soils. Journal of Soil Mechanics and Foundations Division, ASCE, 89(SM1), 39-56.

Hendry, M.T., Sharma, J.S., Martin, C.D., & Barbour, S.L. (2012). Effect of fibre content and structure on anisotropic elastic stiffness and shear strength of peat. Canadian Geotechnical Journal, 49(4), 403-415.

Hobbs, N.B. (1986) Mire morphology and the properties and behaviour of some British and foreign peats. Quart. J. of Eng. Geol., 19: 7-80.

Ishihara K., Tatsuoka F., and Yasuda S. (1975). Undrained deformation and liquefaction of sand under cyclic stresses. Soils Foundations, 15(1), 29–44.

Iwasaki, T., and Tatsuoka, F. (1977). Effects of grain size and grading on dynamic shear moduli of sand. Soils and Foundations, 17(3), 19-35.

Jardine, R.J. (2013). Advanced laboratory testing in research and practice. 2nd Bishop Lecture, 18th Conf. on Soil Mechanics and Geotechnical Engineering, Publisher: Presses des Ponts, 25-55.

Long, M. (2005). Review of peat strength, peat characterisation and constitutive modelling of peat with reference to landslides. Studia Geotechnica et Mechanica, 27(3-4), 67-90.

Kaliakin, V., and Dafalias, Y.F. (1990). Theoretical aspects of the elastoplastic-viscoplastic bounding surface model for cohesive soils. Soils and Foundations, 30(3), 11–24.

Kazemian, S., B.K. Huat, B.B.K., Prasad, A. and Barghchi, M. (2011). A state of art review of peat: Geotechnical engineering perspective. International Journal of the Physical Sciences, 6(8), 1974-1981.

Kramer, S.L. (2000). Dynamic response of Mercer Slough peat. Journal of Geotechnical and Geoenvironmental Engineering, 126(6), 504-510.

Kuwano, R., and Jardine, R.J. (2007). A triaxial investigation of kinematic yielding in sand. Géotechnique, 57(7), 563-579.

Kværner, J., and Snilsberg, P. (2008). The Romeriksporten railway tunnel-drainage effects on peatlands in the lake Northern Puttjern area. Engineering Geology, 101(3), 75-88.

Long, M., and Jennings, P. (2006). Analysis of the peat slide at Pollatomish, County Mayo, Ireland. Landslides, 3, 51–61.

Li, X.S. (2002). A sand model with state-dependent dilatancy. Géotechnique, 52(3), 173-186.

Li, X.S., and Dafalias, Y.F. (2000). A sand model with state-dependent dilatancy. Géotechnique, 50(4), 449-460.

Li, X.S., and Wang, Y. (1998). Linear representation of steady-state line for sand. Journal of Geotechnical and Geoenvironmental Engineering, 124(12), 1215-1217.

Ling, H. I., and Yang, S. (2006). Unified sand model based on the critical state and generalized plasticity. Journal of Engineering Mechanics, 132(12), 1380–1391.

Mesri, G., and Ajlouni, M. (2007). Engineering properties of fibrous peats. Journal of Geotechnical and Geoenvironmental Engineering ASCE, 133(7), 850-866.

Mesri, G., and Choi, Y.K. (1985). Settlement analysis of embankments on soft clays. Journal of Geotechnical Engineering, 111(4), 441-464.

Mesri, G., Stark, T.D., Ajlouni, M.A., and Chen, C.S. (1997). Secondary compression of peat with or without surcharging. Journal of Geotechnical and Geoenvironmental Engineering, 123(5), 411-421.

Nichol, D., and Farmer, I.W. (1998). Settlement over peat on the A5 at Pant Dedwydd near Cerrigydrudion, North Wales. Engineering Geology, 50(3), 299-307.

O'Kelly, B.C., and Zhang, L. (2013). Consolidated-drained triaxial compression testing of peat. ASTM Geotechnical Testing Journal, 36(3), 310-321.

Pichan, S.P. and O'Kelly, B.C. (2012). Effect of decomposition on the compressibility of fibrous peat, ASCE GeoCongress 2012: State of the Art and Practice in Geotechnical Engineering, Oakland, California, USA, 25th–29th March, 2012, edited by R.D. Hryciw, A. Athanasopoulos-Zekkos and N. Yesiller, (GSP 225), 4329 – 4338.

Pichan, S.P., and O'Kelly, B.C. (2012). Stimulated decomposition in peat for engineering applications. Proceedings of the ICE-Ground Improvement, 166(3), 168-176.

Radforth, N.W. (1969). Classification of muskeg. In: MacFarlane, I. C. (ed.) Muskeg engineering handbook. Canadian Building Series. University of Toronto Press.

Richard, F.E., Hall, J.R., Woods, R.D. (1970). Vibrations of soils and Foundations. Prentice-Hall: Englewood Cliffs, NJ, 1970.

Schofield, A.N., and Wroth, C.P. (1968). Critical state soil mechanics, McGraw Hill, London

Shao, Y.F., He, C., Lou, Q.Q. (2007). Stabilization of dredged silt from West Lake. Journal of Jiangsu University (Natural Science Edition), 28(5), 442-445. (in Chinese).

Shu, S. (1090). The request of dredging West Lake in Hangzhou. http://blog.sina.com.cn/s/blog_500bc46501012fe3.html, in Chinese.

Skempton, A. W., & Petley, D. J. (1970). Ignition loss and other properties of peats and clays from Avonmouth, King's Lynn and Cranberry Moss. Géotechnique, 20(4), 343-356.

Smith, P.R., Jardine, R.J., and Hight, D.W. (1992). The yielding of Bothkennar clay. Géotechnique, 42(2), 257-274.

Standard for Soil Test Method (SSTE 1999). National Standard of the People’s Republic of China, GB/T50123-1999. China Planning Press, October 1999.

Wehling, T.M., Boulanger, R.W., Arulnathan, R., Harder, L.F. Jr, and Driller, M.W. (2003). Nonlinear dynamic properties of a fibrous organic soil. Journal of Geotechnical and Geoenvironmental Engineering, 129(10), 929-939.

Wilkinson, S. (2011). The Microstructure of UK Mudrocks, PhD thesis, Department of Civil and Environmental Engineering, Imperial College London.

von Post, L. (1922) Sveriges Geologiska Undersoknings torvinventering och nogra av dess hittils vunna resultat (SGU peat inventory and some preliminary results). Svenska Mosskulturforeningens Tidskrift, Jonkoping, Sweden, 36, 1-37.

Vucetic, M., and Dobry, R. (1988). Degradation of marine clays under cyclic loading. Journal of Geotechnical Engineering, 114(2), 133-149.

Vucetic, M., and Dobry, R. (1991). Effect of soil plasticity on cyclic response. Journal of Geotechnical Engineering, 117(1), 89-107.

Yamaguchi, H., Ohira, Y., Kogure, K., and Mori, S. (1985). Undrained shear characteristics of normally consolidated peat under triaxial compression and extension conditions. Soils and foundations, 25(3), 1-18.

Zhang, L., and O'Kelly, B.C. (2014). The principle of effective stress and triaxial compression testing of peat. Proceedings of the ICE-Geotechnical Engineering, 167(GE1), 40-50.

Zwanenburg, C., den Haan, E.J., Kruse, G.A.M., and Koelewijn, A.R. (2012). Failure of a trial embankment on peat in Booneschans, the Netherlands. Géotechnique, 62(6), 479-490.

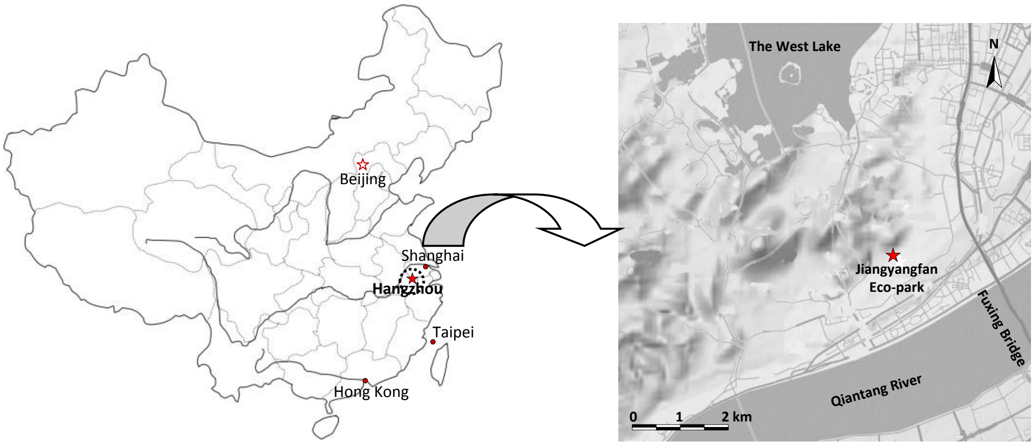

Fig. 1 Maps showing sites of West Lake in Hangzhou and Jiangyangfan Eco-park

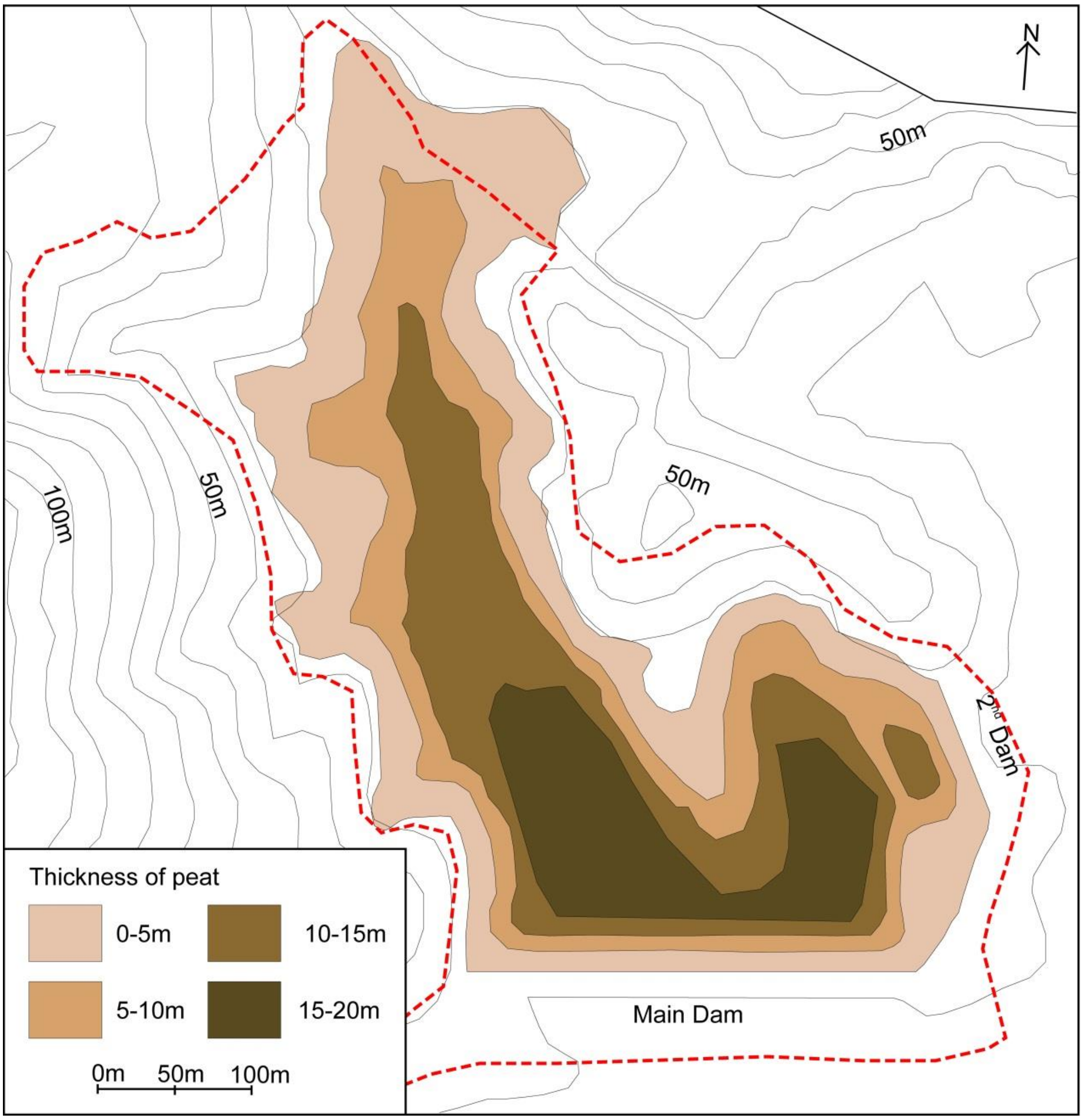

Fig. 2 Contour diagram of thickness of the peat deposited at Jiangyangfan Eco-park

Fig. 3 Chronological aerial views of Jiangyangfan Eco-park site

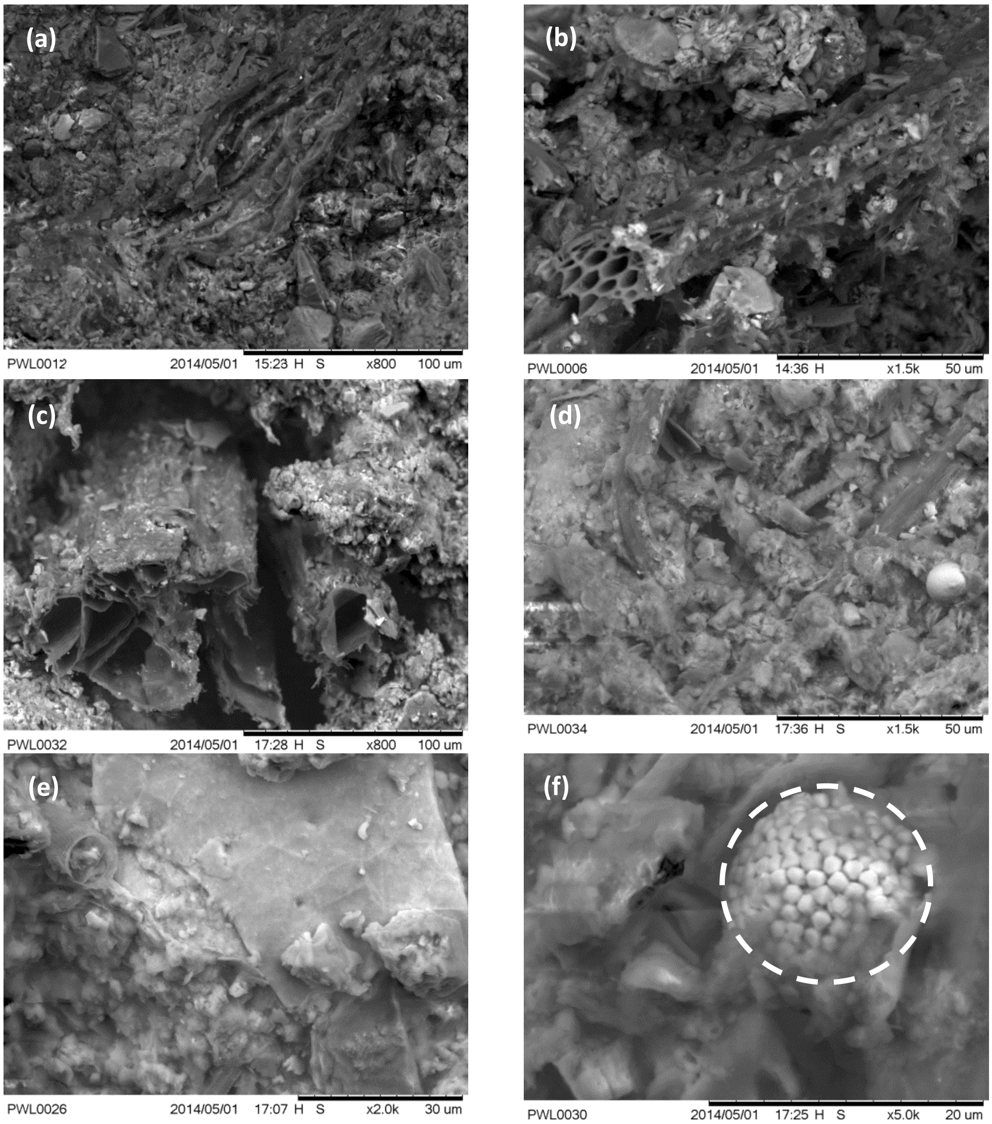

Fig. 4 Scanning electron microscope images of peat samples (a) organic fibres; (b), (c) and (d) stem structures; (e) leaves; (f) pyritic framboids

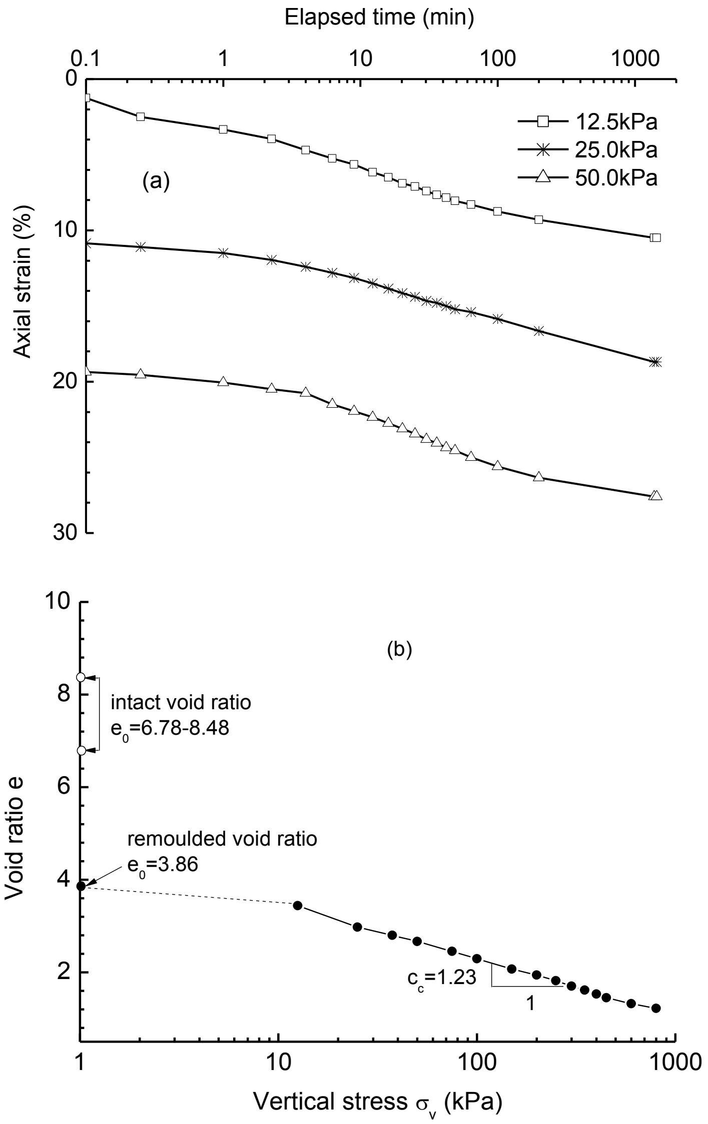

Fig. 5 One-dimensional compression of the WLP

(a) loading increment against elapsed time; (b) e-log(σ_v) curve;

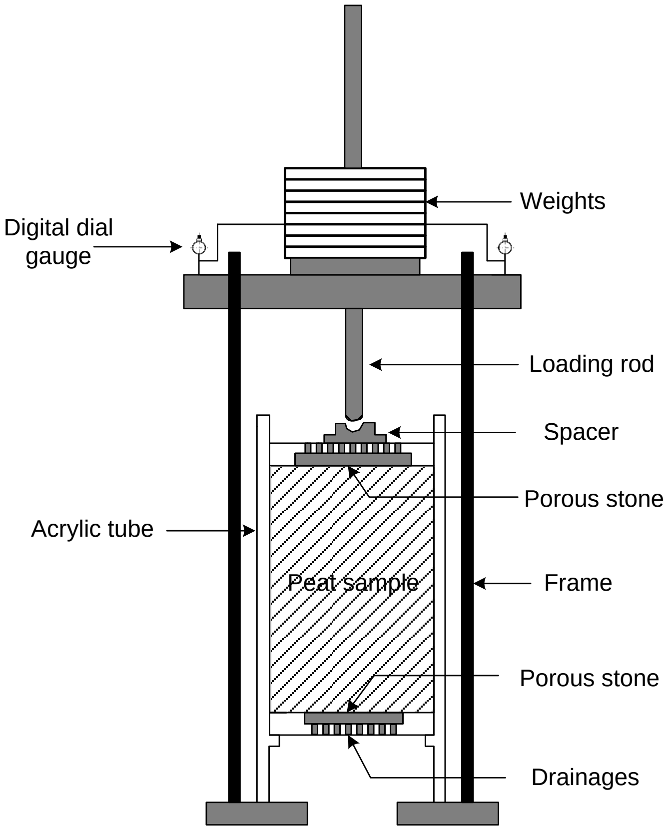

Fig. 6 Schematic drawing of the device for reconstituted sample preparation

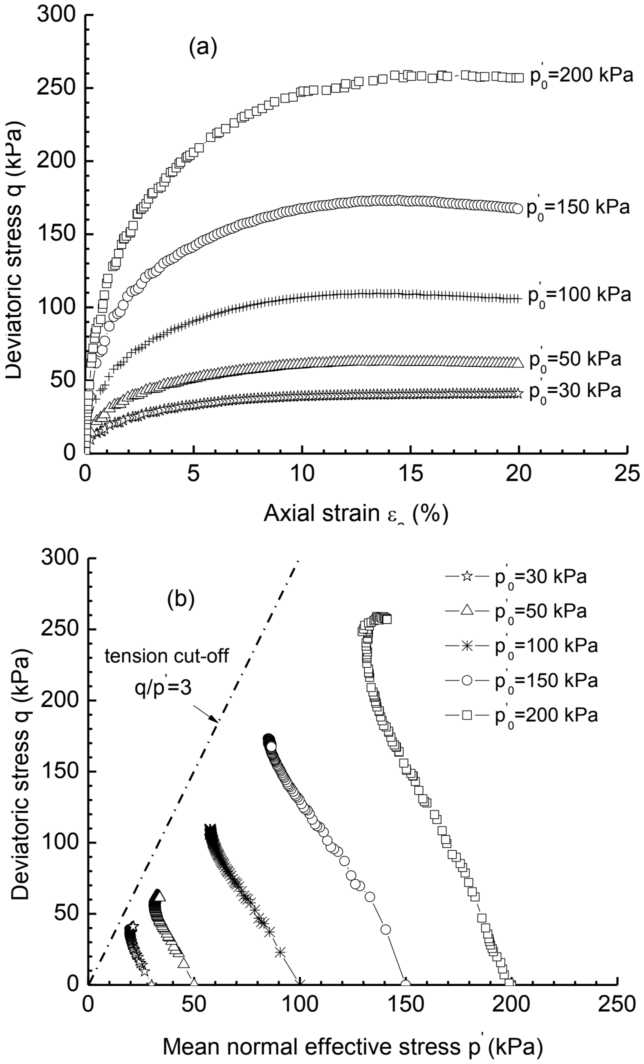

Fig. 7 Triaxial compression tests for peat (a) effective stress paths; (b) stress-strain curves

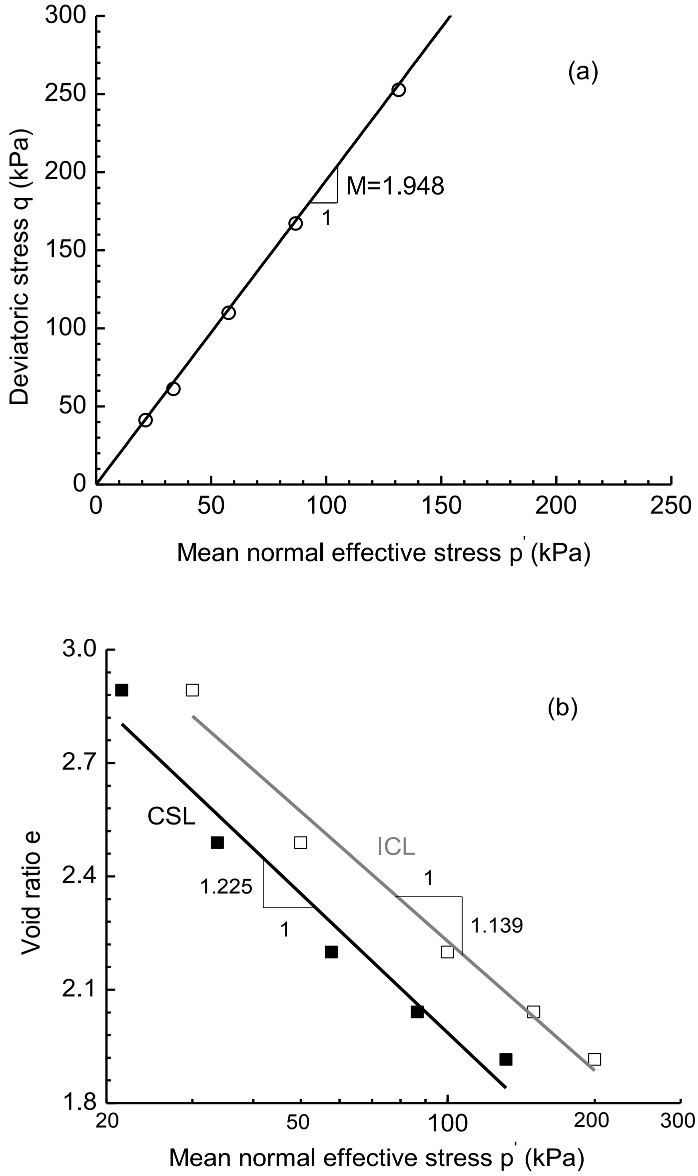

Fig. 8 Critical state line (a) q-p' plane; (b) e-logp' plane

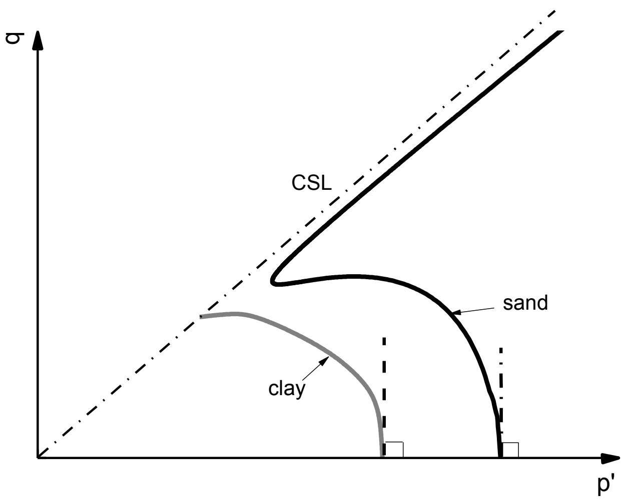

Fig. 9 Typical effective stress paths for sand and normally consolidated clay

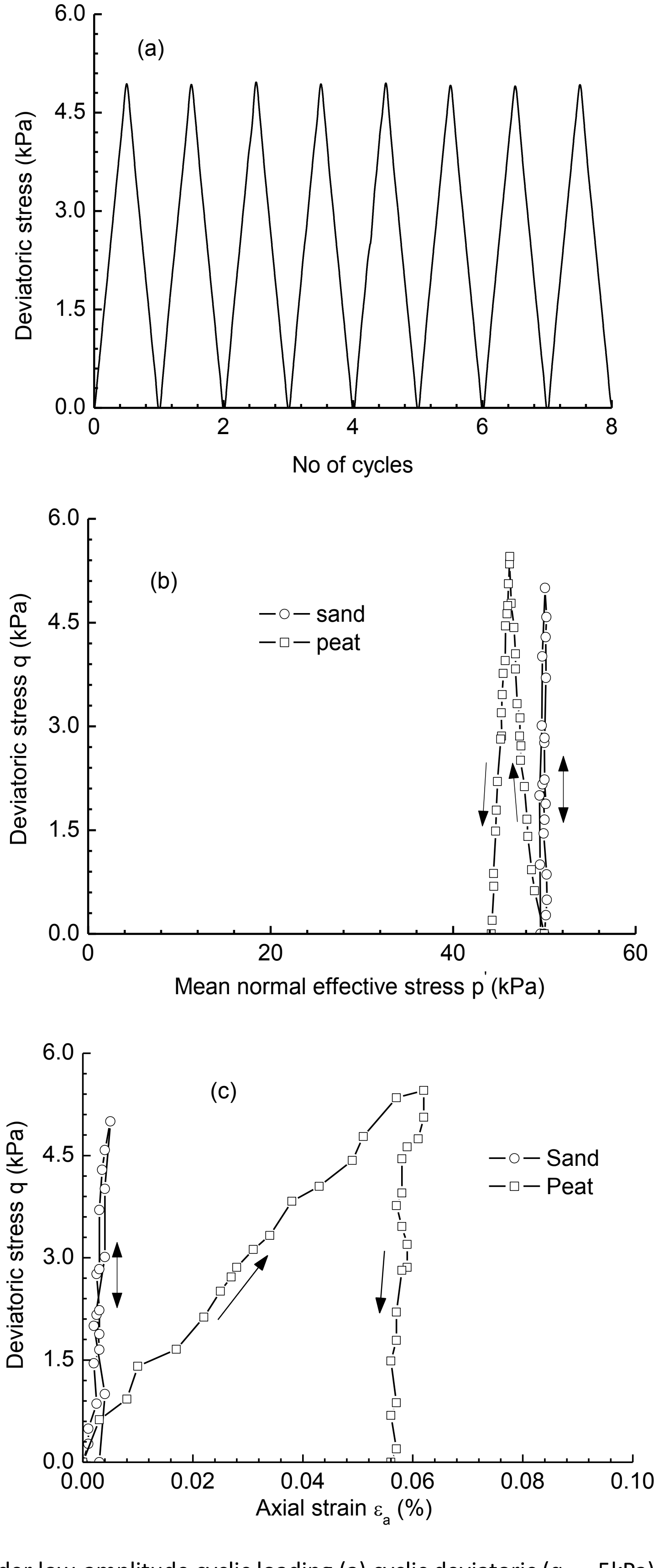

Fig. 10 Peat response under low-amplitude cyclic loading (a) cyclic deviatoric (q_{cyc}=5kPa) loading; (b) 1st cycle response in q-p' plane; (c) 1st cycle response in q-ε_a plane

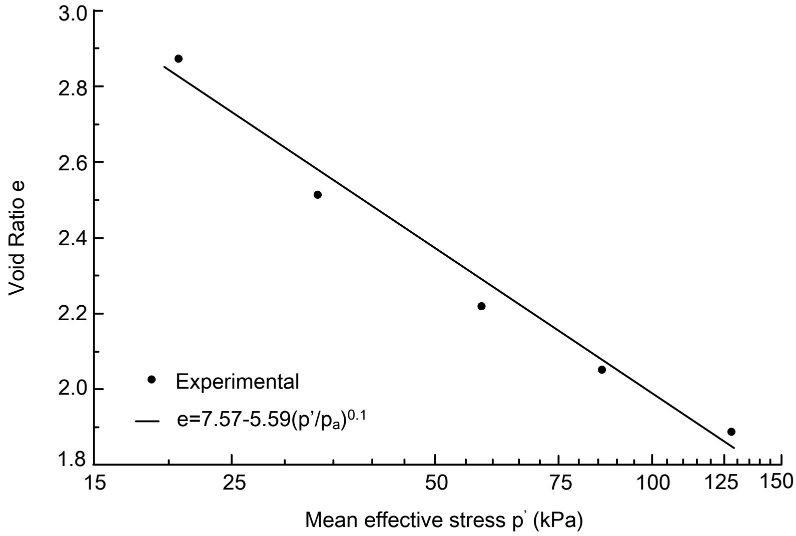

Fig. 11 Linearized critical state line for peat in the constitutive modelling

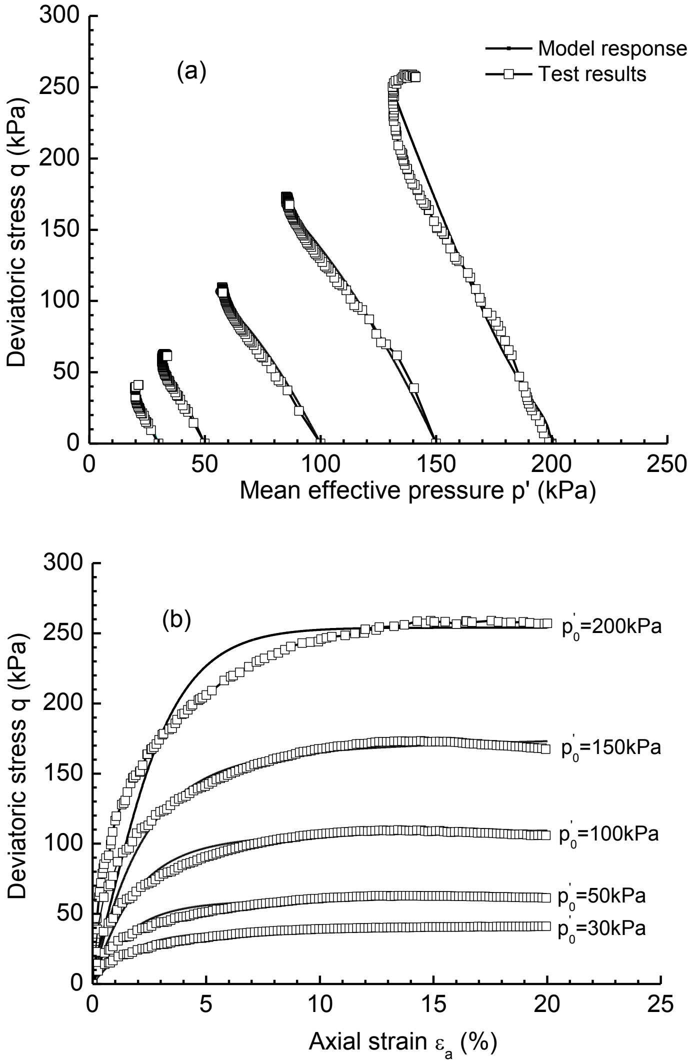

Fig. 12 Comparison between experimental results and model responses for peat
(a) effective stress path; (b) stress-strain curve

Table 1 index properties of West Lake Peat

Natural water content w_0 (%)	Natural bulk density ρ (g/cm^3)	Reconstituted water content w_0 (%)	Specific gravity G_s	Loss on ignition N (%)	Fiber content FC (%) Retained on 63 μm	Fiber content FC (%) Retained on 154 μm	Acidity pH	Permeability k_v (cm/s)
320-400	1.06-1.18	182	2.12	35.0	16.1	4.3	6.4	(2.40-1.83)×10^{-8}

Table 2 Model parameters for West Lake Peat

Elastic Parameters	Critical state parameters	Dilatancy parameters	Hardening parameters
G_0=109 v=0.209	M=1.948 e_Γ=7.57 λ_c =5.59 ξ=0.1	d_0=0.08 m=0.105	h_1=0.587 h_2=0.139 n=0.105